JOURNAL OF Applied Polymer SCIENCE

Thermal and Rheological Effects of Sepiolite in Linear Low-Density Polyethylene/Starch Blend

Sadullah Mir,[1,2,3] Tariq Yasin,[2] Peter J. Halley,[3] Humaira Masood Siddiqi,[1] Orhan Ozdemir,[3] Anh Nguyen[3]

[1]Department of Chemistry, Quaid-i-Azam University, Islamabad, Pakistan

[2]Department of Metallurgy and Materials Engineering, Pakistan Institute of Engineering and Applied Sciences, PO Nilore, Islamabad, Pakistan

[3]Centre for High Performance Polymers, Division of Chemical Engineering, The University of Queensland, Brisbane, Queensland 4072, Australia

Correspondence to: T. Yasin (E-mail: yasintariq@yahoo.com)

ABSTRACT: Effect of different concentrations of sepiolite on thermal and rheological properties of linear low-density polyethylene/starch blend was investigated. Vinyl trimethoxy silane was used as compatibilizing and crosslinking agent. The composites were produced by peroxide-initiated melt mixing technique. Improved thermal stability and tensile strength were observed in crosslinked formulations. Maximum tensile properties were observed in composites containing 2 parts per hundred (phr) sepiolite and 15 phr starch. Rheological study of crosslinked composite showed a linear viscoelastic behavior with high complex viscosity and dynamic shear storage modulus. Scanning electron microscopy also revealed that silane has improved the dispersion of filler and interaction among the polymer and filler interphase. These results suggest that the presence of sepiolite act as an effective filler to enhance the thermal and rheological properties. © 2012 Wiley Periodicals, Inc. J. Appl. Polym. Sci. 000: 000–000, 2012

KEYWORDS: starch; polyethylene; sepiolite; rheology; silane; crosslinking

Received 15 July 2011; accepted 9 March 2012; published online 00 Month 2012
DOI: 10.1002/app.37657

INTRODUCTION

Polyethylene is commercially available in various types and is used as commodity plastic.[1] Its annual production is ~80 million metric tons and mostly used in packaging industry.[2] It is a bio-stable polymer and its growing consumption generates large amount of waste which creates various environmental problems. Its production as plastic bag is banned in many countries. The researchers proposed many solutions to address this issue such as recycling, development of biodegradable polymers, use of biodegradable additives into bio-stable polymers, etc. The plastic post consumer waste can be recycled, but this process is very expensive and the recycled products often have poor properties.[3] Researchers have also developed eco-friendly polymeric materials and products, which are commercialized as biodegradable plastics in various sectors such as packaging, medical, and agriculture.[4-6] But, the synthesis of biodegradable polymer is very tedious and costly job. The consumers are unable to use such expansive products.

Scientists are also trying to develop composites material using biodegradable additives into bio-stable polymers. Natural polymers such as starch, cellulose, and chitosan have been used as biodegradable additives in these composites.[7-9] Starch is a polysaccharide consists of large number of glucose units linked together by glycosidic bonds. It is commercially available and can be easily produced from renewable resources. It has been used as low cost biodegradable additive in polyolefin.[10] The addition of starch as biodegradable additives in polyolefin has certain advantages for example: (1) The time required for degradation of synthetic polymer can be reduced. (2) The quantity of synthetic polymer used can be minimized. (3) The skeleton of the polymer becomes weak, brittle, and degrades more easily. (4) Increased surface area for chemical attack. (5) Promotes microorganism activity. The only drawback of such biodegradable composites is the compatibility of its constituents. Natural polymers are polar in nature while majority of synthetic polymer are nonpolar in nature. Therefore, the resultant composite made from such combination has weak mechanical and thermal properties.[11] For this purpose, different compatibilizing agents have been used. Maleic anhydride has been used by many researchers to enhance the compatibility of starch/polyolefin blends.[12,13]

Similarly, Wang et al. studied the increased compatibility of magnesium hydroxide with low-density polyethylene using dibutyl maleate.[14] Silane containing alkoxy groups has also been used as compatibilizing as well as crosslinking agent. This unique ability of silane has been successfully employed in wood/polyolefins composite.[15]

Sepiolite is a needle-shaped magnesium silicate clay mineral [$Mg_4Si_6O_{15}(OH)_2{\cdot}6H_2O$]. It has been used in polymeric material to improve their thermal and flame-retardant properties.[16,17] It has also been used in small quantity to improve the mechanical properties of polymers.[18,19]

In this work, three approaches were simultaneously used to improve the thermal, mechanical and rheological behavior of linear low-density polyethylene (LLDPE)/starch/sepiolite composite. First, the materials were prepared by peroxide initiated melt mixing technique, which avoids the use of organic solvent. Second, sepiolite was used as supporting filler, which was expected to improve the thermal and mechanical properties. Third, vinyl trimethoxy silane (VTMS) was used as compatibilizing and crosslinking agent to improve the interactions between hydrophilic and hydrophobic components of composites.

EXPERIMENTAL

Materials

LLDPE with melt flow index of 1 g/10 min (190°C/2.16 kg) was purchased from Mitsui Japan. Maize starch (Gelose 80) was obtained from Penford Australia, sepiolite, VTMS, dicumyl peroxide (DCP), dibutyltin dilaurate, and stearic acid were supplied by Sigma-Aldrich, Australia. All the chemicals were used without further purification.

Sample Preparation

The starch was dried in vacuum oven for 24 h at 80°C. The moisture content of starch was measured using Sartorius moisture analyzer and the moisture content before and after drying was 11.7% and 2.1%, respectively. For crosslinked blend, following steps were carried out. The DCP and dibutyltin dilaurate were dissolved in 1.5 mL dry acetone and were sprayed over LLDPE. The DCP-coated LLDPE along with starch, sepiolite, and stearic acid were mixed using Brabender internal mixer for 3 min at 130°C at rotor speed of 33 rpm. VTMS was gradually added to the mixture during melting stage. In the next 7 min, the temperature and the rotor speed were fixed at 170°C and 40 rpm, respectively.

Finally, the mixed material was heat pressed into sheet (1 mm) at 170°C under 50 kN load. The prepared sheets were crosslinked in boiling water at 95°C for 20 h. After crosslinking, the sheets were dried in vacuum oven for 16 h at 70°C before characterization. The compositions of different formulations are shown in Table I.

Characterization

The particle size distribution of sepiolite was determined by Malvern Instrument (Mastersizer 2000) using water as dispersant. Similarly particle size distribution of starch was calculated by using Malvern Instrument (SB.0D) in ethanol (as dispersant medium) rather than water, because starch is soluble in water.

Table I. Formulations Codes of LLDPE/Starch/Sepiolite Composites[a]

Sample code	LLDPE (parts)	Sepiolite (phr)	Starch (phr)
XLS2/15	100	2	15
XLS2/30	100	2	30
XLS2/45	100	2	45
XLS4/15	100	4	15
XLS4/30	100	4	30
XLS4/45	100	4	45
XLS8/15	100	8	15
XLS8/30	100	8	30
XLS8/45	100	8	45

[a]All crosslinked formulations containing DCP 0.15 phr, VTMS 2 phr, DBTDL 0.1 phr, stearic acid 0.03 phr.

Tensile properties were determined using an Instron tensile tester (Model 5543). The instrument was operated at a crosshead speed of 50 mm/min using 5 kN static load cell. The specimens were cut in dumb bell shape (Dimension; Type 4, Standard; ISO 37: 1994) from a 1-mm thick compression molded sheet. Five specimens from each sample were tested.

Differential scanning calorimetry (DSC) studies were performed using DSC Q2000 (TA Instrument). The samples were cut into small pieces and ~5 mg of each sample was used for analysis. To remove the thermal history, the sample was heated from 25°C to 180°C under nitrogen atmosphere. The sample was then cooled to −50°C at 10°C/min and then reheated up to 180°C at 10°C/min and the data of second heating were used to calculate the degree of crystallinity (X_c) using following equation.

$$X_c = (\Delta H_f / \Delta H_f^0) \times 100$$

where ΔH_f and ΔH_f^0 were the enthalpies of the sample and LLDPE, respectively.

The thermal stability of the composites was studied by means of thermogravimetric analysis. The thermogravimetric (TG) experiments were performed using a Mettler Toledo, (TGA/DSC star system) under nitrogen flow of 50 mL/min. Sample of 8-10 mg was heated at a heating rate of 10°C/min from room temperature to maximum of 750°C.

The gel contents of the prepared samples were determined according to ASTM 2765. The samples were cut into small pieces and were placed into stainless steel cloth and weighed. Extraction with *p*-xylene was carried out for 15 h in Soxhlet extractor. The extracted specimens were washed with acetone and then dried to a constant weight under vacuum. Following equation was used to find the gel content of the specimens:

$$\text{Extract} = \frac{\text{Weight loss during extraction}}{\text{Weight of original sample} - \text{Weight of filler}}$$

$$\text{Gel content} = 100 - \text{extract}$$

Time- and temperature-dependent storage modulus (G'), loss modulus (G''), and complex viscosity (η^*) were determined by

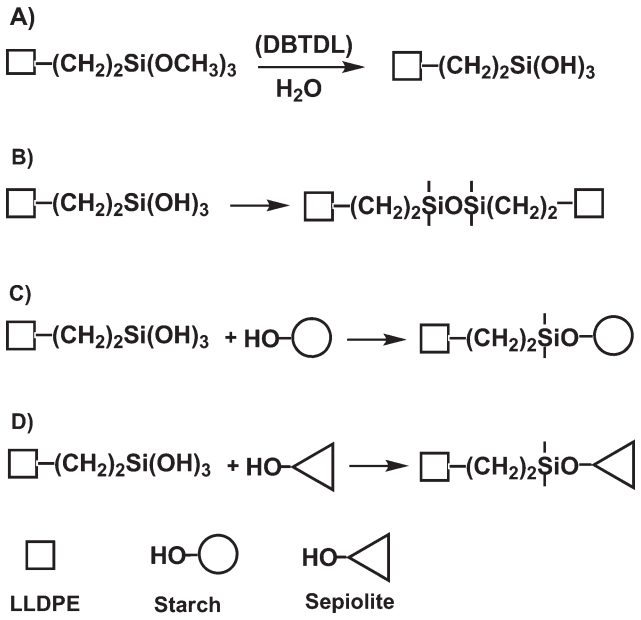

Scheme 1. Reactions during crosslinking: (A) hydrolysis, (B) self-condensation of silanol moieties, (C) condensation of silanol with hydroxyl group of starch, (D) condensation of silanol with hydroxyl group of sepiolite.

an Advance Rheometric Expansion System using parallel plate geometry having plate diameter of 25 mm. The specimens from the compressed molded sheets were cut according to the diameter of the plate. The experiment was performed at 150°C over the frequency range of 0.05 to 100 rad/s. The gap between the plates was automatically adjusted by the instrument.

Scanning electron microscope (Jeol, JSM, 6400F) was used to study the morphology of the prepared samples. Specimens from compress molded sheets were dried overnight in vacuum oven and cryofractured in liquid nitrogen. Carbon fibers were used to coat the cut surfaces. The instrument was operated at 5 kV.

RESULTS AND DISCUSSION

The peroxide induced grafting and crosslinking of polyethylene with vinyl alkoxysilane is a well established and commercialized process. Our group has used silane as compatibilizing and crosslinking agent in different polyolefin composites.[20] The grafting, crosslinking, and compatibilizing reactions of VTMS with polyethylene as well as with starch and sepiolite are shown in Scheme 1.

A. Hydrolysis: The VTMS molecules are hydrolyzed in the presence of water and catalyst yielding reactive silanol groups, as shown in Scheme 1(A).
B. Self-condensation: During the hydrolysis process, the concomitant condensation of silanol groups also takes place, which is termed as self-condensation reaction. These self-condensation reactions of VTMS-grafted polyethylene give crosslinked structure, which increases the crosslinking density of the composites [Scheme 1(B)].
C. Condensation of silanol groups with starch and sepiolite: The silanol groups may also react with hydroxyl groups of starch and sepiolite, and connect the VTMS-grafted polyethylene chains with starch and sepiolite via siloxane bond [Scheme 1(C, D)].

FTIR Analysis

Figure 1(A) shows FTIR spectra of virgin LLDPE (LL) and silane crosslinked LLDPE (XLL) in the spectral range from 3600 to 600 cm^{-1}. Spectrum (i) shows the characteristic absorption bands at 2840 and 2930 cm^{-1}, which correspond to CH_2 stretching modes of vibration of polyethylene. The spectrum (ii) also shows the characteristic absorption band of siloxane Si—O—Si and Si—O—C appeared in the range of 1020–1080 cm^{-1}.[21,22] Additionally, band corresponding to Si—O—Si symmetric vibrations were also observed at 800 cm^{-1}.[21] In Figure 1(B), spectrum (iii) the main absorption bands of starch appearing at 1000, 1150, and 3270 cm^{-1} were assigned to C—O stretching of alcohol bond, C—O stretching of ether bond and

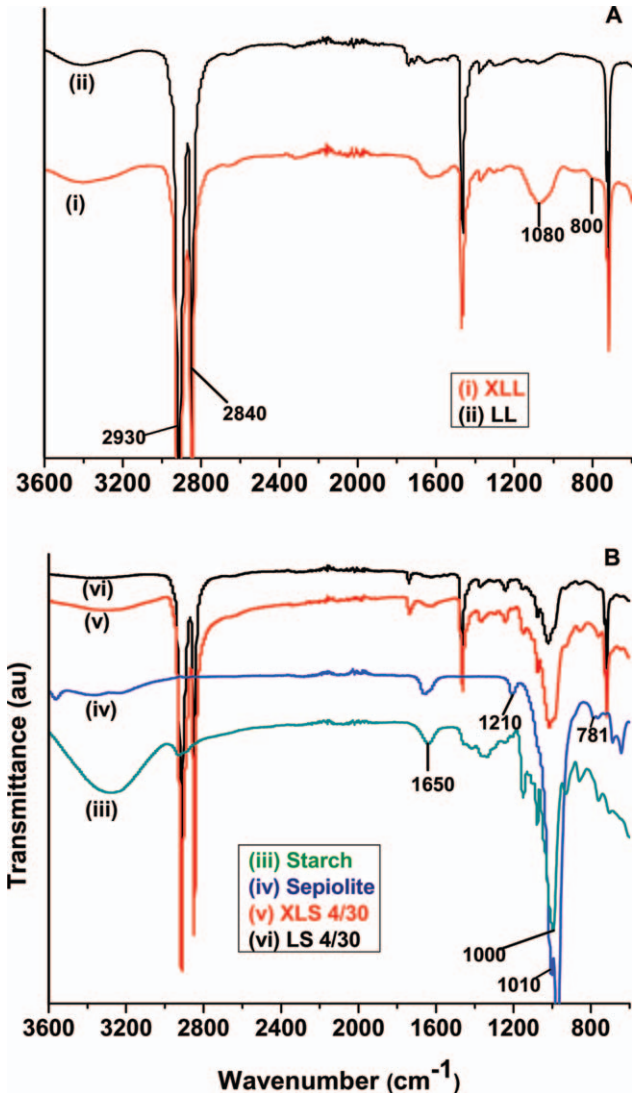

Figure 1. FTIR spectra of XLL (i), LL (ii), starch (iii), sepiolite (iv), XLS4/30 (v), and LS4/30 (vi) in the range of 3600–600 cm^{-1}. [Color figure can be viewed in the online issue, which is available at wileyonlinelibrary.com.]

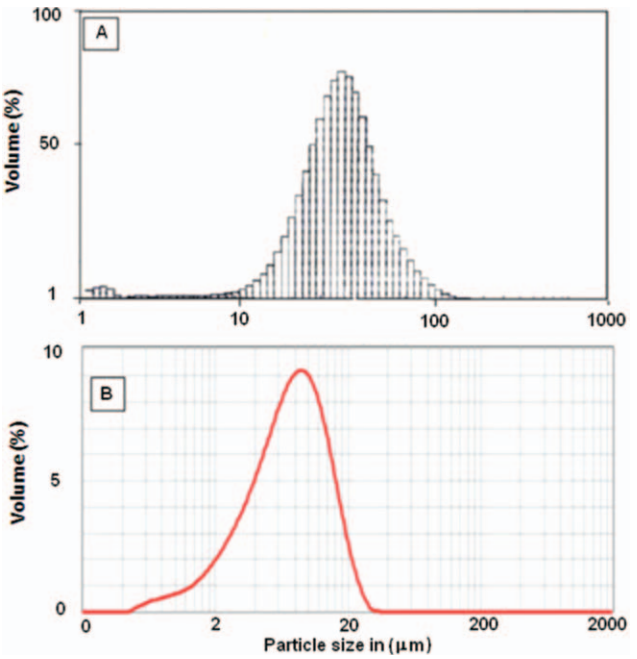

Figure 2. Particle size distribution of starch (A) and sepiolite (B). [Color figure can be viewed in the online issue, which is available at wileyonlinelibrary.com.]

O—H groups, respectively. In spectrum (iv), the characteristic adsorption band of sepiolite appeared at 781, 1010, and 1210 cm^{-1} were attributed to the Si—O—Si, respectively.[23] The important adsorption bands of starch and sepiolite were also found in both non-crosslinked (LS4/30) and crosslinked formulations (XLS4/30) as shown in Figure 1(B) (v, vi) It was observed that the siloxane Si—O—Si and Si—O—C bands was not clearly differentiated in XLS4/30 because sepiolite bands overlap these bands in this region. But the higher intensity of these bands as compared with LS4/30 confirmed this and also supported by the evidence of silane crosslinking reactions from Figure 1(A) (i).

Particle Size Distribution of Starch and Sepiolite

In thermoplastic composites, the particle size of the additives, its distribution and dispersion are vital to understand its rheological, mechanical, and thermal properties. The large particle size of filler/additives and its improper distribution within the matrix usually leads to weak mechanical properties. The particle size distribution of starch and sepiolite are shown in Figure 2. The average particle size of starch varies from 10 to 100 μm. The particles with sizes between 50 and 60 μm consisted of 80% of the total volume. Although the average particle size of sepiolite was in the range of 8 to 10 μm, which contributed more than 90% by volume, the particles with sizes less than 2 μm contributed 20% by volume.

Tensile Properties

Table II summarizes tensile properties of crosslinked and non-crosslinked LLDPE composites. It can be seen from this table that the crosslinked composite has improved tensile strength (TS), whereas elongation at break (E_b) was reduced as compared with noncrosslinked composite. The TS of LS2/30 was 25.5 MPa and that of XLS2/30 was 27.0 MPa. The E_b of this composite was reduced from 720.1% to 635.8% in the crosslinked composite with an overall reduction of 11.8%. Similarly, an improvement of 4.5% in the TS was observed in XLS2/45 and the E_b values were decreased by 12.9%. The high TS and reduced E_b values of crosslinked composite were also reported.[24,25]

The most interesting aspect of the noncrosslinked and crosslinked composite is the reduced TS and E_b values with higher starch loading. The TS of 30-phr starch loading of LS2/30 and XLS2/30 was dropped by 16.6% and 15.7% relative to the composite having 15-phr starch loading. Similarly, at 45-phr starch loading, the TS values of LS2/45 and XLS2/45 were further decreased by 32.4% and 31.4%, respectively. The E_b values of both non-crosslinked and crosslinked composite also showed similar decreasing trend with high starch loading.

The sepiolite loading also affects the tensile properties of these composite. It was observed that TS and E_b of both non-crosslinked and crosslinked composite decreased with increasing sepiolite loading. The lowest TS was observed for LS8/45, which is 17.5 MPa with lowest E_b (465.3%). The tensile properties were decreased when sepiolite and starch loading were increased to 8 and 45 phr, respectively. Maximum TS and E_b values were observed in composites containing 2-phr sepiolite and 15-phr starch.

DSC

The melting temperature (T_m), heat of fusion (ΔH_f), and percentage crystallinity (X_c) of composite is shown in Table III. This table shows negligible changes in T_m values of both non-

Table II. Tensile Properties of LLDPE/Starch/Sepiolite Composites

Samples	T_b (MPa)	E_b (%)	Samples	T_b (MPa)	E_b (%)
LS2/15	30.6 ± 0.4	771 ± 1	XLS2/15	32.0 ± 0.3	687 ± 1
LS2/30	25.5 ± 0.3	720 ± 1	XLS2/30	27.1 ± 0.2	635 ± 1
LS2/45	20.7 ± 0.2	635 ± 1	XLS2/45	21.9 ± 0.4	553 ± 2
LS4/15	29.7 ± 0.4	710 ± 1	XLS4/15	30.3 ± 0.3	640 ± 1
LS4/30	23.4 ± 0.2	659 ± 1	XLS4/30	25.0 ± 0.5	590 ± 2
LS4/45	18.8 ± 0.3	610 ± 1	XLS4/45	20.4 ± 0.5	539 ± 1
LS8/15	27.9 ± 0.4	646 ± 1	XLS8/15	29.2 ± 0.2	603 ± 1
LS8/30	22.4 ± 0.3	583 ± 1	XLS8/30	24.1 ± 0.4	506 ± 2
LS8/45	17.4 ± 0.5	559 ± 1	XLS8/45	19.2 ± 0.4	465 ± 1

Table III. DSC Analysis of LLDPE/Starch/Sepiolite Composites

Sample	T_m (°C)	ΔH_f (J/g)	X_c (%)	Sample	T_m (°C)	ΔH_f (J/g)	X_c (%)
LS2/30	121.2	75.90	25.9	XLS2/30	120.3	75.09	25.6
LS2/45	120.8	66.14	22.5	XLS2/45	120.5	60.14	20.5
LS4/30	121.2	74.20	25.3	XLS4/30	121.1	72.01	24.5
LS4/45	121.1	65.28	22.2	XLS4/45	120.7	63.86	21.7
LS8/30	121.3	75.30	25.6	XLS8/30	121.0	73.58	25.1
LS8/45	121.5	64.38	21.9	XLS8/45	121.2	59.66	20.3

crosslinked and crosslinked composites. All the crosslinked composites have slightly lower X_c as compared with non-crosslinked composites. The lowering of X_c of crosslinked composites was associated to the network formation resulting from the addition of crosslinker, which reduced the chain flexibility.[26] Similar behavior has been observed in thermoplastic wood composites.[27]

Similarly, the amount of starch and sepiolite also affect T_m and X_c. At higher starch and sepiolite loading the X_c and T_m values showed decreasing trend. The maximum X_c was observed in LS2/30 which was 25.9%, whereas LS8/45 showed the minimum value of X_c, i.e. 21.9%. These results show that greater quantity of additives inhibits the close packing of LLDPE which in turn reduces the percentage crystallinity of the composites.

Thermogravimetric Analysis

Figure 3 shows TGA thermograms and Table IV shows percentage mass loss of composites at various temperature ranges. Both the non-crosslinked and crosslinked composites showed two-stage degradation behavior, but the crosslinked curves showed improved thermal stability as compared with non-crosslinked composites.

The first stage of degradation up to 400°C mainly corresponded to decomposition of starch. Starch is a thermally less stable polymer as compared with polyethylene and its degradation involved dehydration, ring scission, and decomposition reactions.[28] The second mass loss above 400°C was attributed to the decomposition of LLDPE, which involved C—C and C—H bond breakage.

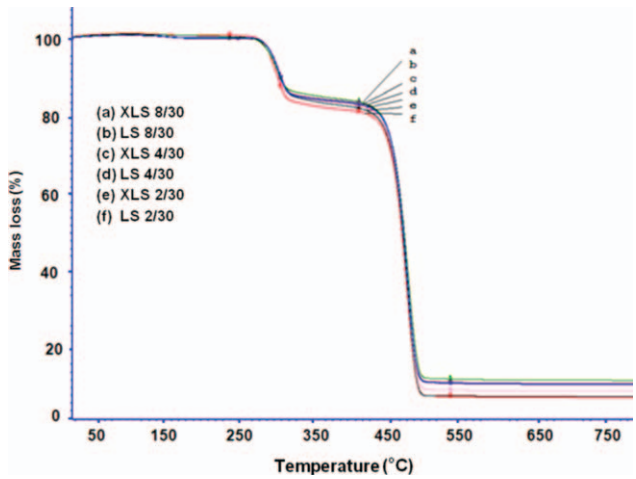

Figure 3. TGA thermograms of LLDPE/starch/sepiolite composites. [Color figure can be viewed in the online issue, which is available at wileyonlinelibrary.com.]

Table IVshows major mass losses at temperatures 311 and 418°C and the residue left at temperature 542°C. At these temperatures, slightly low mass losses and higher weight residues were observed for crosslinked samples. This higher thermal stability of crosslinked composites is due to silane crosslinking and to the amount of filler loading.

Gel Content Analysis

Table V shows the gel content of crosslinked composites. It is evident that percentage crosslinking increases gradually with increasing amount of starch in the composites. The highest degree of crosslinking was observed for the composite with 45-phr starch loading. This behavior can be explained on the basis of the possible condensation reactions of silanol group with starch and sepiolite which increase at higher filler loading.

The effect of sepiolite loading on gel content of these composites can also be seen from this table. First, the gel content value increases up to 4-phr sepiolite loading and then drops at 8-phr sepiolite loading. The lowering of gel content at this loading might be due to utilization of silanol group by sepiolite. Therefore, the number of available silanol groups for the crosslinking of the polyethylene-grafted silane is drastically reduced.

Melt Rheology

Figure 4 shows dynamic shear storage modulus (G') of both non-crosslinked and crosslinked composites. Both the composites showed normal behavior at lower frequency, i.e. the crosslinked formulations showed higher G' values than non-crosslinked composite. This increase in G' values of the crosslinked composites is attributed to the elastic nature. The anomalous

Table IV. Percentage Mass Loss and Residue of LLDPE/Starch/Sepiolite Composites

Sample	Mass loss (%)[a]	Mass loss (%)[b]	Residue (%)[c]
LS2/30	12.11	18.66	7.46
XLS2/30	9.59	17.73	7.55
LS4/30	10.77	17.04	9.09
XLS4/30	9.58	16.49	11.09
LS8/30	10.27	16.73	10.90
XLS8/30	9.79	16.10	11.98

[a]At 311°C., [b]At 418°C., [c]At 542°C.

Table V. Gel Content Analysis of LLDPE/Starch/Sepiolite Composites

Sample	Gel content (%)	Sample	Gel content (%)	Sample	Gel content (%)
XLS2/15	18.2	XLS2/30	27.4	XLS2/45	35.2
XLS4/15	24.6	XLS4/30	31.3	XLS4/45	41.6
XLS8/15	16.1	XLS8/30	20.0	XLS8/45	29.4

behavior of crosslinked XLS4/30 at higher frequency is associated to its higher gel content, whereas at lower frequency, both increase in crosslinking and amount of filler tend to increase the G' values of XLS8/30. This increase in G' values of both non-crosslinked and crosslinked composites with increasing frequency are related to molecular chain relaxation phenomena. At higher frequency, the entangled chains have short time to relax back thus an increase in the G' values were observed.[29]

Figure 5 indicates the dynamic shear loss modulus also called viscous modulus (G'') curves of non-crosslinked and crosslinked composite. The G'' curves of the non-crosslinked composite are well above the crosslinked composites, indicating the weak interaction among the components. In all composites, G'' increased with increasing frequency and with the quantity of fillers.

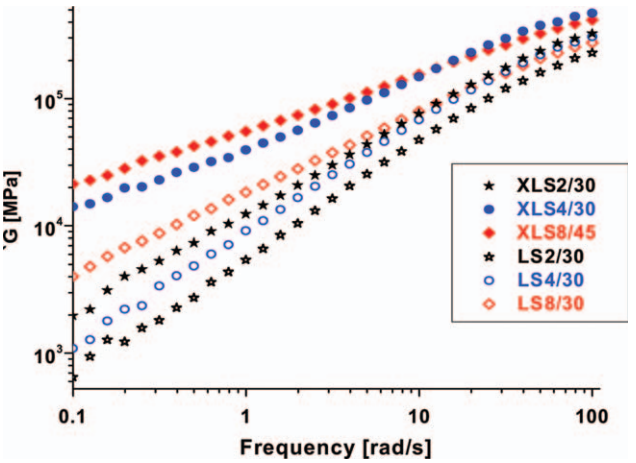

Figure 4. Dynamic shear storage moduli (G') of LLDPE/starch/sepiolite composites. [Color figure can be viewed in the online issue, which is available at wileyonlinelibrary.com.]

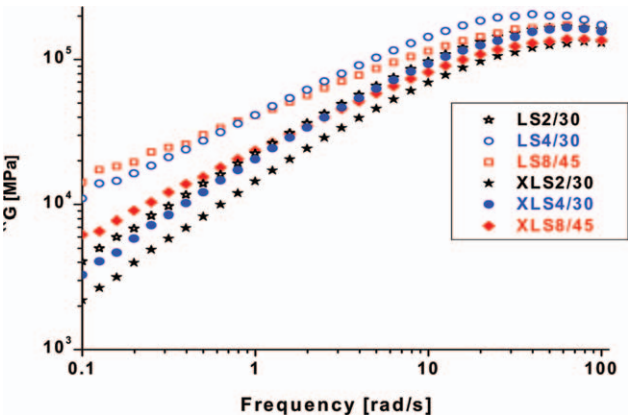

Figure 5. Dynamic shear loss moduli of LLDPE/starch/sepiolite composites. [Color figure can be viewed in the online issue, which is available at wileyonlinelibrary.com.]

Figure 6 shows complex viscosity (η^*) of non-crosslinked and crosslinked composites. The crosslinked composites showed higher η^* attributed to the formation of network structure which offered greater resistance to the applied stresses. The η^* of both non-crosslinked and crosslinked composites also depends upon the amount of filler. The higher filler loading showed higher η^* values for both types of composites. Moreover, η^* is also frequency dependent and decreases with increasing operating frequency. This behavior is called shear thinning effect at molten state[29].

SEM Analysis

Figure 7 shows scanning electron micrographs of non-crosslinked and crosslinked composition. These images show uniform distribution of starch and sepiolite in the LLDPE matrix. Dispersion and distribution of the filler in the matrix play a vital role and affect the mechanical properties of the resultant composite.

In non-crosslinked composites LS2/30 (A), LS4/30 (C) and LS8/30 (E), some gaps were observed showing poor adhesion among the components, whereas in crosslinked composites (B, D, F) the filler particles are well embedded in the polymer matrix and no gaps were observed. This improved compatibility and adhesion among the filler–matrix interphase are attributed to the silane coupling agent. Some fine particles of sepiolite were also observed both in non-crosslinked and crosslinked composites.

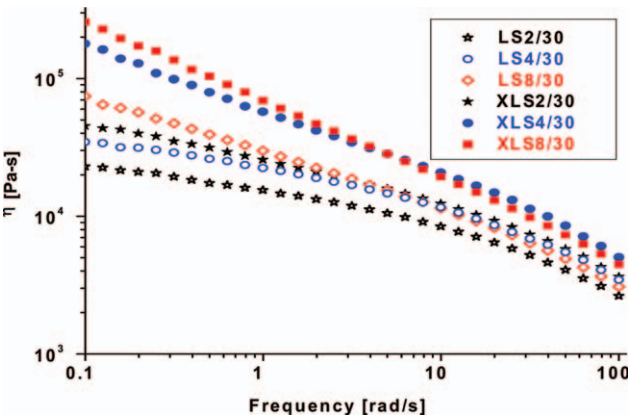

Figure 6. Complex viscosities (η^*) of LLDPE/starch/sepiolite composites. [Color figure can be viewed in the online issue, which is available at wileyonlinelibrary.com.]

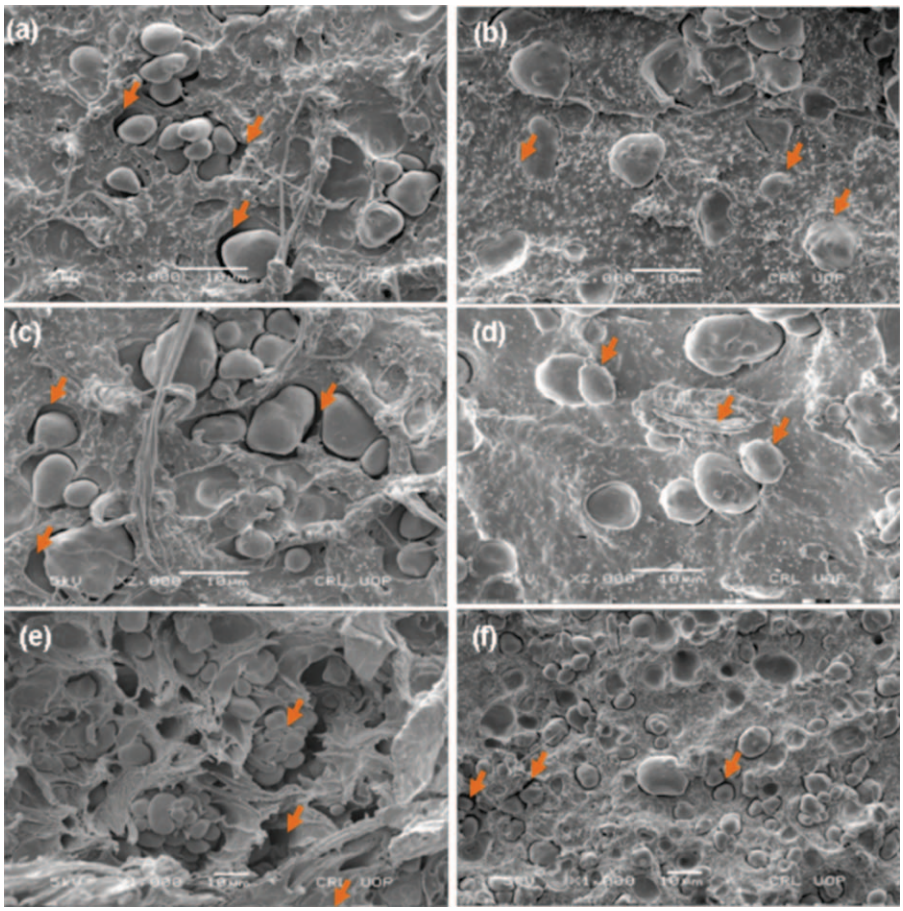

Figure 7. SEM micrographs of LLDPE/starch/sepiolite composites: LS2/30 (A), XLS2/30 (B), LS4/30 (C), XLS4/30 (D), LS8/30 (E), and XLS8/30 (F). [Color figure can be viewed in the online issue, which is available at wileyonlinelibrary.com.]

These smaller particles are evenly distributed in the matrix and can support the larger starch particles during applied mechanical stresses thus acting as supporting filler.

The weak mechanical properties of LS8/30 and XLS8/30 can also be explained through SEM micrographs. The non-crosslinked LS8/30 shows aggregation of filler particles, which strongly interact with each other through hydrogen bonding and have weak interaction with polymer matrix. The reduced interaction between the starch and LLDPE causes weak mechanical properties. In XLS8/30, there is uniform dispersion of the starch particles, which resulted higher mechanical properties as compared with XLS8/30.

CONCLUSIONS

In conclusion, the properties of LLDPE/starch/sepiolite composites can be improved by using VTMS as crosslinking and compatibilizing agent. The maximum TS values were observed for the crosslinked composite with reduced E_b values. However, the TS and E_b values of non-crosslinked and crosslinked composite showed a reduced trend with increasing starch and sepiolite loading. Percentage crystallinity of crosslinked composites was lowered due to the disorder in close packing of polyethylene matrix as well as by the formation of network structure. Both non-crosslinked and crosslinked composites showed similar degradation behavior. But, the crosslinked composites showed higher thermal stability. The gel contents were directly proportional to the amount of starch loading because at higher starch loading the probability of condensation and dehydration reactions were increased. The dynamic shear moduli and complex viscosities of crosslinked composites were higher than non-crosslinked composites. The anomalous behavior of crosslinked XLS4/30 at higher frequency is associated to its higher gel content. In XLS8/45, at lower frequency, both crosslinking and the amount of filler increase G' values. The SEM image of non-crosslinked composites showed clear gaps between the polymer and fillers which indicates poor adhesion among the components whereas the crosslinked composites are quite stable and the filler particles are well embedded in the polymer matrix. This behavior indicates a strong interaction between the filler–matrix interphase.

ACKNOWLEDGMENTS

The author (Mr. Sadullah Mir) wishes to thank Higher Education Commission of Pakistan for financial assistance and grateful to the Center of High Performance Polymer University of Queensland, Australia for technical support.

REFERENCES

1. Kahlen, S.; Wallner, G. M.; Lang, R. W. *Solar Energy* **2010,** *84*, 1577.
2. Piringer, O. G.; Baner, A. L. Plastic packaging: interactions with food and pharmaceuticals, Wiley-VCH: Weinheim, **2008.**
3. Tzankova, D. N.; La Mantia, F. P. *Polym. Adv. Technol.* **1999,** *10*, 607.
4. Bucci, D. Z.; Tavares, L.B. B.*; Sell, I.* Polym. Test. **2005,** *24*, 564.
5. John, C. M.; Arthur, J. T. *Biomaterials* **2000,** *21*, 2335.
6. Briassoulis, D. J. *Polym. Degrad. Stabil.* **2006,** *91*, 1256.
7. Meera, K.; Sun-Ja, L. *Carbohydr. Polym.* **2002,** *50*, 331.
8. Mir, S.; Yasin, T.; Halley, P. J.; Siddiqi, H. M.; Nicholson, T. *Carbohydr. Polym.* **2011,** *83*, 414.
9. Tajeddin, B.; Rahman, R. A.; Abdulah, L. C. *Int. J. Bio. Macromol.* **2010,** *47*, 292.
10. Nawang, R.; Danjaji, I. D.; Ishiaku, U. S.; Ismail, H.; Mohd, I. Z. *A.* Polym. Test. **2001,** *20*, 167.
11. Ramkumar, D. H. S.; Mrinal, B.; Utpal, R. V. *Eur. Polym. J.* **1997,** *33*, 729.
12. Chandra, R.; Rustgi, R. *Polym. Degrad. Stabil.* **1997,** *56*, 185.
13. Bikiaris, D.; Prinos, J.; Koutsopoulos, K.; Vouroutzis, E. N.; Pavlidou, N.; Frangis, C. *Polym. Degrad. Stabil.* **1998,** *59*, 287.
14. Wang, Z. Z.; Qu, B. J.; Fan, W. C.; Hu, Y. A.; Shen, X. F.; *Polym. Degrad. Stabil.* **2002,** *76*, 123.
15. Bengtsson, M.; Oksman, K. *Comp. Sci. Technol.* **2006,** *66*, 2177.
16. Bilotti, E.; Fischer, H. R.; Peijs, T. J. *Appl. Polym. Sci.* **2008,** *107*, 1116.
17. Gul, R.; Yasin, T.; Islam, A.; Mir, S. J. *Appl. Polym. Sci.* **2011,** *121*, 2772.
18. Bokobza, L.; Burr, A.; Garnaud, G.; Perin, M. Y.; Pagnotta, S. *Polym. Int.* **2004,** *53*, 1060.
19. Shafiq, M.; Yasin, T.; Saeed, S. J. *Appl. Polym. Sci.* **2012,** *123*, 1718.
20. Xie, Y.; Hill, C.A. S.; Xiao, Z.; Militz, H.; Mai, C. *Composites Part A: Appl. Sci. Manuf.* **2010,** *41*, 806.
21. Magnus, B.; Oksman, K. Composites Part A: *Appl. Sci. Manuf.* **2006,** *37*, 752.
22. Wang, Z. Z.; Hu, Y.; Gui, Z.; Zong, R. W. *Polym. Test.* **2003,** *22*, 533.
23. Wang, K. W.; Tseng, P. C.; Chang, S. S.; Ray, D. T, Shau, Y. H.; Shen, Y. W.; Chen, R. C.; Chiang, P. N. *Clays Clay Miner.* **2009,** *57*, 521.
24. Balsuriya, P. W.; Ye, L.; Mai, Y. W.; Wu, J. J. *Appl. Polym. Sci.* **2002,** *83*, 2505.
25. Jang, B.C.; Huh, S.Y.; Jang J.G; Bae, Y.C. *J. Appl. Polym. Sci.* **2001,** *82*, 3313.
26. Mathot, V.B. F. *Polymer* **1984,** *25*, 579.
27. Magnus, B.; Baillif, M. L.; Kristiina, O. *Comp. A* **2007,** *38*, 1922.
28. Rasool, N.; Yasin, T.; Akhter, Z. *e-Polymers* **2008,** *142*, 1.
29. Baghaei, B.; Jafari, S. H.; Khonakdar, H. A.; Rezaeian, I.; As'habi, L.; Ahmadian, S. *Polym. Bull.* **2009,** *62*, 255.